Kenneth P. Roberts[1]
Cheng-H. Lin[1]
Maria Singhal[2]
George P. Casale[2]
Gerald J. Small[1]
Ryszard Jankowiak[1]

[1]Ames Laboratory – USDOE and Department of Chemistry, Iowa State University, Ames, IA, USA
[2]Eppley Institute for Research in Cancer and Allied Diseases, University of Nebraska Medical Center, Omaha, NE, USA

On-line identification of depurinating DNA adducts in human urine by capillary electrophoresis – fluorescence line narrowing spectroscopy

The benzo[*a*]pyrene (BP)-derived 7-(benzo[*a*]pyren-6-yl)guanine (BP-6-N7Gua) depurinating one-electron oxidation adduct was identified in the urine extracts of coal-smoke-exposed humans for the first time. Urine samples were prepared by solid-phase extraction and reversed-phase high-performance liquid chromatography. Subsequently, the BP-6-N7Gua adduct was identified on-line with capillary electrophoresis - fluorescence line narrowing spectroscopy (CE-FLNS) at 4.2 K. The daily excretion of BP-6-N7Gua in human urine of individuals exposed to coal smoke was approximately 226 pmol per μmol of creatinine. Due to the high level of excretion we propose that BP-6-N7Gua adducts found in urine could serve as effective biomarkers for risk assessment of BP exposure. The results demonstrate that CE-FLNS allows for on-line separation and DNA adducts identification in complex fluid extracts.

Keywords: Depurinating DNA adducts / Capillary electrophoresis / Fluorescence line narrowing / Analyte identification / One-electron oxidation EL 3811

1 Introduction

Capillary electrophoresis (CE) is now a well-established and widely used analytical and bioanalytical separation technique. Various protocols necessary for CE separation of molecular analytes have been established [1–4]. Using CE, polycyclic aromatic hydrocarbon (PAH) carcinogens were measured with a detection level of 0.1 amol [5]. CE has also been successfully applied to the analysis of DNA adducts [3, 6–9], nucleic acid bases, and DNA oligonucleotides [2]. Fluorescence line narrowing spectroscopy (FLNS) provides frequency selection by exciting a homogeneous ensemble of molecules, providing a means to overcome the inhomogeneous spectral broadening [10, 11]. FLNS is capable of distinguishing between a given PAH metabolite covalently bound to different DNA bases and to different nucleophilic centers of a given base [10–14]. Furthermore, FLNS has been used to distinguish between a given metabolite bound in helix external, partially base-stacked, and intercalated conformations [10, 11, 15]. Subfemtomole detection limits have been obtained, *i.e.* ~one adduct in 10^8 base pairs can be measured in about 100 μg of DNA [16]. Although excellent selectivity and sensitivity of FLNS indicate that this methodology is a powerful tool for the study of both stable and depurinating DNA adducts [10–17], note that a complex mixture of closely related adducts/metabolites cannot be resolved by FLNS alone.

Therefore, we recently demonstrated that CE can be interfaced with FLNS for on-line structural characterization. It was shown that detection by laser-induced fluorescence (LIF) under line narrowing (FLN) conditions provided excellent spectral resolution, which allowed for structural characterization of various PAHs [4] and PAH-derived DNA adducts [3, 8, 9]. We emphasize that CE-FLNS does not require standards each time the analytes are identified. Rather, it relies on an established reference library of spectra. This attribute is particularly important when standards (*e.g.*, DNA adducts/metabolites) are difficult/expensive to synthesize, and/or exhibit poor stability. We have also shown that adduct identification can be achieved with CE-nonline narrowing (NLN) fluorescence spectroscopy at 4.2 K [3] (or at 77 K; unpublished results). For NLN spectroscopy, nonselective excitation into the S_2 state with a single-frequency excitation source can be used, leading to excitation of all sites within the inhomogeneously broadened band. The resulting spectra are much more characteristic for analyte identification than room temperature spectra. With this approach expensive tunable lasers are not required, thus expanding the applicability of low temperature LIF detection in CE [3].

Benzo[*a*]pyrene (BP), the carcinogen of interest in this manuscript, can be activated by one-electron oxidation to yield reactive intermediate radical cations and by monooxygenation to produce bay-region diol epoxides [17–21].

Correspondence: Dr. Ryszard Jankowiak, Ames Laboratory USDOE, Iowa State University, 706 Gilman Hall, Ames, IA 50011, USA
E-mail: jankowiak@ameslab.gov
Fax: +515-294-1699

Abbreviations: BP, benzo[*a*]pyrene; **BP-6-N7Ade**, 7-(benzo[*a*]-pyren-6-yl)adenine; **BP-6-N7Gua**, 7-(benzo[*a*]pyren-6-yl)guanine; **DOSS**, sodium dioctyl sulfosuccinate; **FLNS**, fluorescence line narrowing spectroscopy; **NLN**, nonline narrowing; **PAH**, polycyclic aromatic hydrocarbon

0173-0835/00/0404-0799 $17.50+.50/0

The active intermediates formed by one-electron oxidation and monooxygenation readily bind to DNA and have been shown to form adducts *in vitro* and *in vivo* [18, 22]. Results obtained in recent years unequivocally demonstrated the importance of the one-electron oxidation pathway for the carcinogenic activation of PAHs [18]. For example, it was shown that the BP-radical cation (at the C6 position) binds *in vitro* to the N7 position of adenine or guanine to form unstable 7-(benoz[*a*]pyren-6-yl)adenine (BP-6-N7Ade) and 7-(benzo[*a*]pyren-6-yl)guanine (BP-6-N7Gua) adducts that are rapidly lost (depurinated) from DNA [21, 23]. Mouse skin studies showed that the major BP-derived depurinating adducts formed are BP-6-N7Ade, BP-6-N7Gua, and BP-6-C8Gua; together, they account for 74% of all BP adducts formed [22, 24–26]. The presence of the BP-6-N7Gua adduct was also demonstrated in urine and feces of rats exposed to BP, where the identification was made by off-line FLNS [21]. However, the question remains whether or not these adducts are formed in humans.

In this study, urine from coal-smoke-exposed individuals is analyzed by CE-FLNS for the presence of BP-DNA adducts, since BP is one of the major carcinogens found in coal smoke [27]. Previously, PAH metabolites such as 1-hydroxypyrene-glucuronide and BP-tetraols were used as biomarkers of PAH exposure in urine assays of individuals exposed to coal tar [28]. However, identification of depurinated PAH-DNA adducts in human fluids, if formed at detectable levels, would be more relevant indicators of PAH exposure since they directly reflect PAH-induced DNA damage.

2 Materials and methods

Caution. BP is an extremely hazardous chemical and should be handled carefully in accordance with NIH guidelines.

2.1 Materials

Sodium tetraborate (STB), sodium dioctyl sulfosuccinate (DOSS), and dimethyl sulfoxide (DMSO) were obtained from Aldrich (Milwaukee, WI). Acetonitrile (ACN), methanol, and sodium hydroxide (NaOH) were obtained from Fisher Scientific (Fair Lawn, NJ). All buffers were prepared with water purified by a NANOpure II (Barnstead, Dubuque, IA) purification system. Capillaries were 75 μm ID, 375 μm OD UV-transparent bare silica purchased from Polymicro Technologies (Phoenix, AZ). BP-6-N7Gua and BP-6-N7Ade standards were prepared *via* iodine oxidation reaction of BP with the individual DNA bases as described in detail elsewhere [18].

2.2 CE-FLNS instrumentation

The CE-FLNS instrumentation is described in [3, 5, 6]. Briefly, the system consists of a modular CE system (Crystal 300 series, Model 310, ATI Unicam, Boston, MA), FLNS apparatus, and a capillary cryostat (CC). A schematic of the CE-FLN/FNLN system is shown in Fig. 1. The CC consists of a double-walled quartz cell with inlet and return lines for introducing liquid nitrogen or liquid helium. The outer portion of the CC is evacuated. The capillary, positioned in the central region of the CC, is

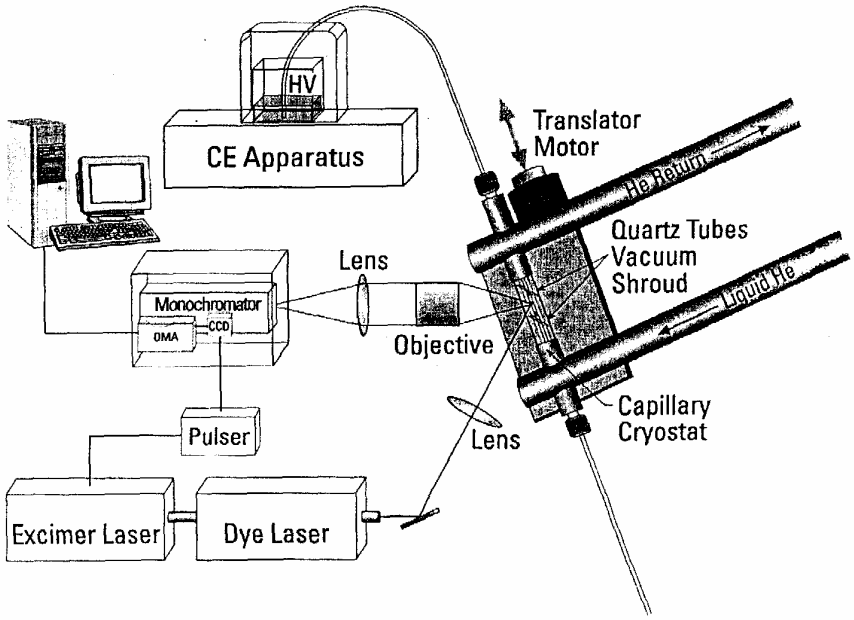

Figure 1. Schematic apparatus of the CE-FLNS system used for low temperature structural identification of CE-separated analytes.

cooled by a continuous flow of liquid nitrogen (77 K) or liquid helium (4.2 K). The low thermal capacity of the capillary and the small dimensions of the CC (inner portion, 4 mm ID × 22 cm length) allow rapid cooling to 4.2 K (in less than 1 min) and the ability to form disordered matrices for FLN to be operative in typical CE buffers. A precision stage provides translation of the CC along the capillary axis by ± 4 cm, allowing the separated analytes to be sequentially characterized by LIF spectroscopy. Room-temperature LIF electropherograms were obtained with a CW excitation source (Model Innova 90C argon ion laser; Coherent, Santa Clara, CA) equipped with UV optics and an intracavity prism for single line selection. The excitation wavelength was 351.1 nm with an output power of 100 mW. Fluorescence was collected with a reflecting objective (25-0506 × 15, Ealing, Holliston, MA; numerical aperture of 0.28), passed through a Model 218 0.3 m monochromator (McPherson, Acton, MA), and detected with an intensified charge-coupled device (ICCD) (Roper Scientific, Trenton, NJ). The FLN spectra were obtained with a Lambda Physik FL-2002 pulsed dye laser, pumped by a Lambda Physik Lextra 100 XeCl excimer laser (Lambda Physik, Fort Lauderdale, FL). Low-temperature spectra were obtained using gated and nongated modes of detection. A gate width of 200 ns and various delay times, as specified in the figure captions, were used. Spectral resolution for NLN fluorescence and FLN spectra was 0.8 and 0.05 nm, respectively.

2.3 Solid-phase extraction (SPE) and reversed-phase high-performance liquid chromatography (RP-HPLC)

The (dominantly) hydrophobic BP-derived adducts/metabolites from human urine were isolated by a multi-staged process (Casale *et al.*, in preparation). Urine samples were standardized to 100 mg creatinine as an internal standard. Extraction and preconcentration methods were employed with urine to minimize a large number of the (unwanted) endogenous species, which can chemically and spectrally interfere with the analytes of interest. The procedure was established with the extraction of adduct standards (BP-6-N7Gua and BP-6-N7Ade) added to human urine. The C-18 chains of the SPE cartridge efficiently retained the hydrophobic species, while a majority of unwanted components present in the urine samples (*e.g.*, salts) eluted without retention. Adducts were released from the Sep-Pak columns when the 60/40 v/v% point was reached on the elution gradient. The standards were further isolated with a chloroform extraction, followed by evaporation to a volume of 10 μL. Then 200 μL DMSO was added and evaporation continued until the chloroform was removed. Based on the RP-HPLC (C-18) retention times established by BP-6-N7Gua/-N7Ade standards, maximum sample clean-up was achieved when 10 min (70–80 min retention window) eluate fractions were collected from the first HPLC separation (methanol/water gradient). After concentrating the effluent to 200 μL in DMSO, urine samples were further purified with the second RP-HPLC (ACN/water gradient) separation. With this separation, optimal adduct isolation (*i.e.*, maximum adduct recovery with minimal background components) was achieved by collecting a 10 min fraction (30–40 min retention window) established by the adduct standards. Finally, effluent collected from the second separation was concentrated to 30 μL in DMSO for CE-FLNS analysis.

2.4 CE separation conditions

The CE buffer consisted of a 15% v/v ACN solution containing 20 mM DOSS, and 4 mM sodium tetraborate. Aqueous NaOH was used to adjust the pH to 9. Before injection, the separation buffer was filtered through a 0.22 μm syringe filter (Costor) and then degassed for 5 min. All CE experiments were carried out in the micellar electrokinetic chromatography (MEKC) mode [29]. Introduction of the organic modifier ACN to the separation buffer provided adduct solubility within the mobile phase and thus established the dynamic equilibrium needed for differential partitioning (resolution) of the analytes by the pseudostationary phase. Capillaries (85 cm in length with 75 cm effective length) were conditioned with 100 mM NaOH for 15 min (30 min for new capillaries), water for 5 min, and separation buffer for 15 min. The samples were hydrodynamically injected with 20 mbar pressure for 3 s, resulting in an approximately 10 nL injection volume. Electrokinetic separations were carried out at 22 kV, resulting in a current of ~19 μA. To eliminate the possibility of contamination of adduct standards, room-temperature CE-LIF was used to confirm the purity of BP-6-N7Gua and B-6-N7Ade adduct.

2.5 Off-line FLNS experiments

Reference spectra of BP-derived adduct standards were performed in 100% CE buffer. The samples were placed in 2 mm ID quartz tubes, and brought to 4.2 K in a double nested liquid helium dewar for LIF measurements under NLN and FLN conditions. Approximately 20 μL sample volumes were sufficient for off-line analyses. The delay times and gate widths are specified in figure captions.

2.6 Molecular modeling

Molecular structures of BP-6-N7Gua and BP-6-N7Ade are shown in Fig. 2. Structural optimization of one of these adducts (–N7Gua) was performed with Hyper-

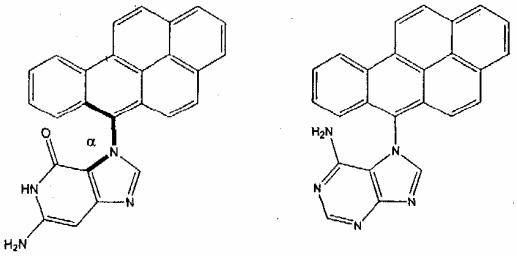

Figure 2. Molecular structures of one-electron oxidation BP-6-N7Gua and BP-6-N7Ade adducts. The dihedral angle α corresponds to rotation around the single bond that connects the two moieties.

Chem's molecular modeling program. The MM+ force field parameters developed for organic molecules and the Polak-Ribiere method for molecular mechanics optimization were employed. A quenched dynamics (*i.e.*, simulated annealing) was used to explore the conformational space. Ten structures were minimized and then subjected to 100 ps of molecular dynamics at $T = 400$ K. The dihedral angle α, defining the relative orientation of guanine in respect to the BP-moiety (see Fig. 2), was used as a variable during the exploration of the conformational space. A Monte Carlo method was employed to determine the average value of α. Ten simulations were performed with 2000 steps at $T = 400$ K with a maximum allowed atomic displacement of 0.05 Å. Fifteen randomly selected structures were again subjected to a 100 ps run (at 400 K) and cooled to 0 K in 2 ps. The (0,0) transitions were calculated for the resulting fifteen structures using the ZINDO/S semiempirical quantum mechanical method.

3 Results and discussion

3.1 Separation of BP-6-N7Gua and BP-6-N7Ade: limit of detection

The room-temperature fluorescence electropherogram of the expected depurinated adducts standards (10^{-8} M) is shown in Fig. 3. Peaks a and b correspond to BP-6-N7Gua and BP-6-N7Ade, respectively, as established by CE migration times. The small unidentified peaks observed in the electropherogram of Fig. 3 most probably correspond to adduct decomposition products, and/or impurities present in solvents used in purification and/or CE separation. The inset of Fig. 3 shows the CE electropherogram obtained for the BP-6-N7Ade standard at much lower concentration. Fluorescence was integrated in the 385–500 nm range. This result establishes an absolute limit of detection for the BP-6-N7Ade adduct (at room temperature) of approximately 2 amol (~2×10^{-10} M; S/N ~~3); the detection limit for BP-6-N7Gua was similar.

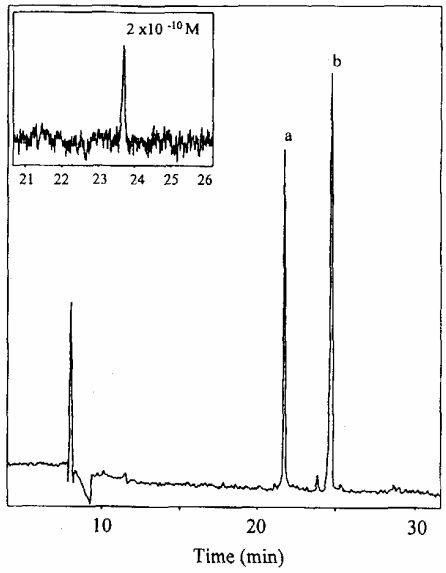

Figure 3. CE electropherogram of the BP adduct standards. Peak a corresponds to BP-6-N7Gua and peak b to BP-6-N7Ade. The small (unidentified) peaks in the electropherogram are presumed to be impurities and/or adduct decomposition products. Inset, a detection limit of 10^{-10} M is shown for the BP-6-N7Ade standard. Laser excitation wavelength, 351.1 nm; power output set to 100 mW. The fluorescence intensity of the electropherogram was obtained by integration of the spectral region from 385–500 nm.

3.2 Identification and relative abundance of BP-6-N7Gua in human urine

Curve a of Fig. 4 shows the CE separation of the 10 min HPLC urine fraction (see Section 2.3) of an individual chronically exposed to coal smoke (*i.e.*, ~30 μg of BP per day). Electropherograms b and c are those of the BP-6-N7Gua standard and a urine fraction from a nonexposed individual, respectively. The data, based on migration times and standard additions, indicate that the intense peak (~23 min) in the electropherogram of the coal-smoke-exposed individual (curve a) corresponds to BP-6-N7Gua at a level of ~0.9 fmol. No detectable amounts of the BP-6-N7Gua or BP-6-N7Ade were observed in the electropherogram of the urine extract from the nonexposed individual (curve c).

Figure 5 shows another example of an electropherogram (left) of a urine fraction from a second coal-smoke-exposed individual. In addition to the electropherogram, NLN fluorescence spectra of the CE separated peaks were monitored in real-time. An intense peak at ~23 min (labeled with an asterisk) is also observed for this individual. The 4.2 K NLN spectrum of this peak is indistinguishable from that of the BP-N7Gua standard, suggesting

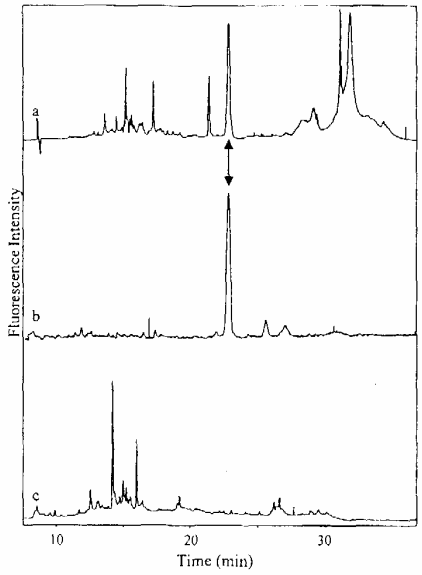

Figure 4. CE separations of (a) urine extract of an individual exposed to coal smoke, (b) BP-6-N7Gua standard, and (c) the urine extract of a nonexposed individual. The arrow marks the location of the depurinated adduct, BP-6-N7Gua. The fluorescence intensity of the electropherogram was obtained by integration of the spectral region from 385–500 nm. Spectra were obtained with an excitation wavelength of 351.1 nm (output power of 100 mW).

again that BP-6-N7Gua is formed *in vivo*. The same quantitation procedure as described above revealed that the level of BP-6-N7Gua is ~0.6 fmol. It is worth pointing out that the peaks at ~13 and 16 min, with emission maxima at ~475 and ~430 nm, would likely prevent spectral characterization of the ~23 min peak had the analysis been performed using off-line NLN fluorescence. No attempts were made to identify the peaks whose spectra do not resemble BP-type fluorescence.

3.3 CE-FLNS analysis

The results in Fig. 5 indicate that the one electron oxidation BP-6-N7Gua adduct is probably formed in humans. Nevertheless, a more definitive identification is required. The 4.2 K NLN spectrum of the CE-separated peak (~23 min), obtained with an excitation wavelength of 351.1 nm, is shown in Fig. 6A. The spectrum is indistinguishable from that of the BP-6-N7Gua adduct standard (spectrum not shown). We note that at 4.2 K the fluorescence intensity increases by a factor of 10 due to the higher fluorescence quantum yield. The latter along with longer detection times for the frozen and stationary analyte zone provides subattomole detection limit. Figure 6B shows the 4.2 K high resolution on-line FLN spectrum

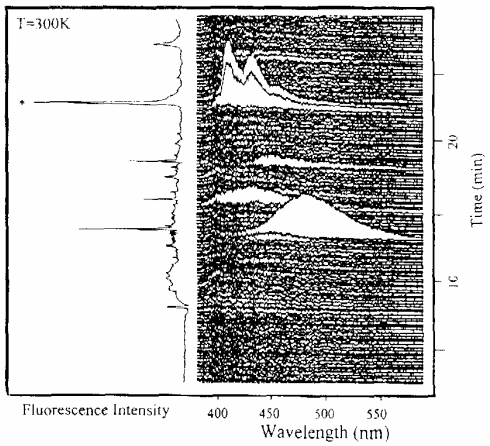

Figure 5. CE electropherogram, with fluorescence spectra corresponding to the CE-separated peaks obtained for urine extract from an individual exposed to coal smoke (λ_{ex} = 351.1 nm). Fluorescence intensity of the electropherogram (left) was obtained by integration of the spectral region from 385–500 nm. The peak labeled with an asterisk correspond to the BP-6-N7Gua adduct (see Section 3.2 for details).

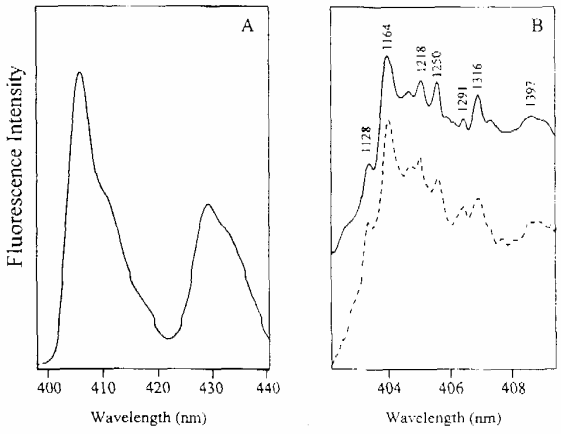

Figure 6. On-line 4.2 K analysis of the CE-separated peak at ~23 min in the electropherogram of Fig. 5. (A) NLN fluorescence spectrum of the CE-separated peak obtained with a CW Ar-ion laser 351.1 nm. The origin, or (0,0)-band, is at 406 nm. (B) Comparison of the on-line FLN spectrum (solid line) for the CE separated peak to the FLN spectrum of BP-6-N7Gua standard. The FLN peaks are labeled with their excited-state vibrational frequencies, in cm^{-1}. T = 4.2 K; λ_{ex}, 386.5 nm, gate width, 200 ns with a 40 ns delay.

(λ_{ex} = 386.5 nm) for the CE-separated peak (solid line) and the off-line FLN spectrum (dashed line) of the BP-6-N7Gua standard. The FLN spectra are nearly indistinguishable as revealed by the identical frequencies (and intensities) of the excited state vibronic modes at 1128, 1164, 1218, 1250, and 1316 cm^{-1}. This result provides

conclusive proof that the DNA adduct is BP-6-N7Gua and, as well, underscores the high selectivity and sensitivity of CE-FLNS.

Quantitative studies revealed that the daily excretion of BP-6-N7Gua by the two individuals studied in this work was about 200 pmol per day. From spiking experiments, it was determined that adduct recovery was 65–85%; therefore, the daily excretion could be ~18–53% higher. In terms of the creatinine level (an internal standard), the two coal-smoke-exposed individuals excreted about 226 pmol of BP-6-N7Gua per µmol of creatinine. By way of comparison, it was recently shown that psoriasis patients treated with coal tar medication excreted (in urine) 5–250 pmol of 1-hydroxypyrene [30] and 15.0 ± 29.5 pmol of BP-tetraols per (µmol of creatinine [28]. The BP tetraols were claimed to be relevant for PAH cancer risk assessment because formation of BP diolepoxide (which is known to form stable DNA adducts) precedes formation of BP tetraols [31]. 1-Hydroxypyrene (the metabolite most often used to assess PAH exposure) was measured in the urine of garbage incineration workers at the level of 0.05–0.41 pmol per (µmol of creatinine [32]. However, we believe, due to the relatively high abundance of the BP-6-N7Gua adduct formed in coal-smoke-exposed humans, that it is a more biologically relevant marker for PAH exposure since it reports directly on DNA damage.

3.4 Spectral characterization of the BP-6-N7Gua standard

The 4.2 K fluorescence origin bands of BP-6-N7Gua in CE separation buffer obtained under NLN conditions are shown in Fig. 7A. The origin band maximum for 0 ns delay is at 407.1 nm shifting to 406.1, 405.6, 404.5 nm for 20, 40 and 80 ns delay times, respectively. The gate width was kept constant at 20 ns. Such a blue shift with increasing delay time has been observed for the BP-6-N7Ade adduct and was attributed to a distribution of BP-6-N7Ade adduct conformers [33].

Vibronically excited FLN spectra (Fig. 7A, curves a–c), obtained with λ_{ex} = 386.5 nm and delay times of 0, 40, and 80 ns are shown in Fig. 7B. The observed narrowing of the FLN spectra and decreasing intensity of the zero-phonon lines in the long wavelength region with increasing delay time indicates that fluorescence originates only from BP-6-N7Gua adducts absorbing at the high-energy wing of the inhomogeneously broadened vibronic absorption band. The latter is in agreement with the observed distribution of fluorescence lifetimes (data not shown). Such narrowing correlates well with the NLN spectra shown in Fig. 7A. From an analytical standpoint, the

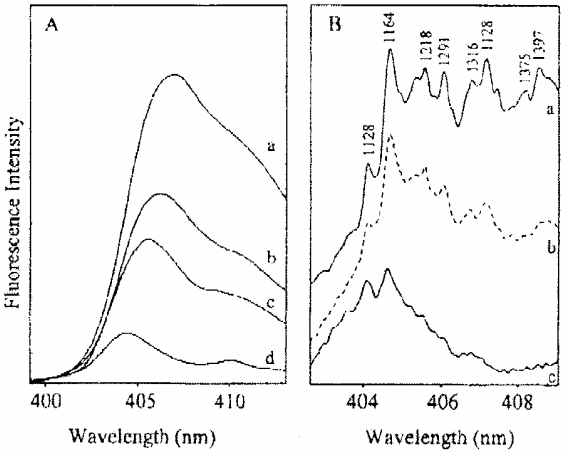

Figure 7. (A) NLN fluorescence spectra (curves a–d) of BP-6-N7Gua in CE buffer obtained at delay times of 0, 20, 40, and 80 ns, respectively; λ_{ex} = 308 nm. Spectra b, c, and d were multiplied by a factor of 2, 8, and 40, respectively. (B) FLN spectra obtained for BP-6-N7Gua in CE buffer with an excitation wavelength of 386.5 nm for 0 (spectrum a), 40 (spectrum b), and 80 ns (spectrum c) delay times. The numbers correspond to excited-state vibrational frequencies in cm^{-1}. *T*, 4.2 K; gate width, 200 ns.

importance of the results is that adducts formed *in vivo* and corresponding adduct standards should be measured with identical delay times.

3.5 Modeling studies of BP-6-N7Gua

To provide some insight on the blue-shift of the fluorescence origin bands, a molecular modeling study was initiated. A typical structure obtained from molecular dynamics simulations (T = 0 K), and subsequent optimization, is shown in Fig. 8. The dihedral angle α (defined in Fig. 2) of the optimized BP-6-N7Gua structure at T = 0 K is 90.2°. Monte Carlo simulations performed at 400 K revealed that the average value of α over the whole simulation period was ~91° with a root-mean-square (RMS) deviation of ~6°. This suggests that, upon cooling to 4.2 K, a distribution of conformations with slightly different α values is possible. As a check on this, fifteen randomly selected and thermally equilibrated (at 400 K) structures of BP-6-N7Gua were subjected to additional quenched dynamics to see whether or not a distribution of α exists at 0 K. The calculations revealed a narrow distribution of dihedral angles with α equal to 91.5° ± 1.4°.

Results of the ZINDO/S calculations on the fifteen structures showed that the mean (0,0)-transition was at 397.0 nm with an RMS of ± 0.5 nm. The experimentally observed (0,0)-band for BP-6-N7Gua in ethanol and CE

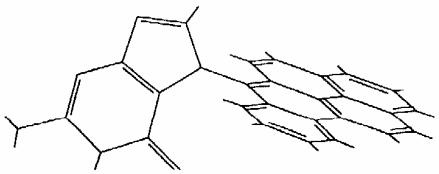

Figure 8. Optimized structure of the BP-6-N7Gua adducts. The average value of α is 90.2° at $T = 0$ K.

buffer glasses was red-shifted by ~8 nm and ~9 nm, respectively; this discrepancy is primarily due to the fact that the calculations were performed *in vacuo*. Since we are interested in the relative energy shift rather than absolute values, the calculated RMS deviation of ± 0.5 nm for the selected conformers can be compared with experimental results. The results show that the RMS deviation of the (0,0)-bands is in reasonable agreement with the experimental data where the relative band shifts are ~1.6 nm for the CE buffer (see Fig. 7A) and 1.2 nm for an ethanol glass (results not shown), respectively. However, this agreement might be fortuitous since the blue shift could also originate from a matrix-induced change in the relative orientation between the two moieties and/or frequency-dependent permanent dipole moment changes across the inhomogeneously broadened absorption band.

4 Concluding remarks

CE-FLNS was used to prove that the depurinating adduct BP-6-N7Gua is formed in humans. The urine fractions analyzed were isolated by SPE and RP-HPLC. Attomole detection limits with CE-FLNS were demonstrated and quantitative studies revealed that the level of BP-6-N7Gua formed in humans exposed to coal smoke was ~200 pmol per day (~226 pmol per μmol of creatinine). The identification of BP-6-N7Gua in humans provides further support for the hypothesis that the one-electron oxidation metabolic pathway plays an important role in PAH-induced carcinogenesis. It is possible that the formation of apurinic sites and stable BP diolepoxide-type adducts work in concert to prevent error-free repair of DNA. Be that as it may, it is reasonable to assume that there is considerable positive correlation between the levels of apurinic sites and stable adducts formed. Thus, the characterization and determination of depurinating PAH-DNA adducts in urine provides a basis for risk assessment monitoring. This approach is more reliable than one based on the monitoring of PAH metabolites produced by detoxification pathways since it reports DNA damage directly.

Ames Laboratory is operated for the U.S. Department of Energy by Iowa State University under contract No. W-7405-Eng-82. The Office of Health and Environmental Research supported this research. Support to C.-H. Lin, G. Casale, and M. Singhal was provided by the NCI, grant PO1 CA49210. The authors thank Dr. J. Mumford (US Environmental Protection Agency, National Health and Environmental Effects Research Laboratory; Epidemiology and Biomarker Branch, Research Triangle Park, NC 27711) for urine samples, and Dr. E. L. Cavalieri (Eppley Institute for Research in Cancer, University of Nebraska Medical Center, Omaha, NE) for providing the BP-6-N7Gua and BP-6-N7Ade adduct standards.

Received July 26, 1999

5 References

[1] Yan, C., Dadoo, R., Zhao, H., Zare, R. N., Rakestraw, D. J., *Anal. Chem.* 1995, *67*, 2026–2029.

[2] Milofsky, R. E., Yeung, E. S., *Anal. Chem.* 1993, *65*, 153–157.

[3] Roberts, K., Lin, C.-H., Jankowiak, R., Small, G. J., *J. Chromatogr. A* 1999, *853*, 159–170.

[4] Jankowiak, R., Zamzow, D., Ding, W., Small, G. J., *Anal. Chem.* 1996, *68*, 2549–2553.

[5] Nie, S., Dadoo, R., Zare, R. N., *Anal. Chem.* 1993, *65*, 3571–3575.

[6] Barry, J. P., Norwood, C., Vouros, P., *Anal. Chem.* 1996, *68*, 1432–1438.

[7] Deforce, D. L. D., Ryniers F. P. K., Van den Eeckhout, E. G., Lemiere, F., Esmans, E. L., *Anal. Chem.* 1996, *68*, 3575–3584.

[8] Zamzow, D., Lin, C.-H., Small, G. J., Jankowiak, R., *J. Chromatogr. A* 1997, *781*, 73–80.

[9] Zamzow, D., Small, G. J., Jankowiak, R., *Mol. Cryst. Liq. Cryst.* 1996, *291*, 155–162.

[10] Jankowiak, R., Cooper, R. S., Zamzow, D., Small, G. J., Doskocil, G., Jeffrey, A. M., *IARC Scientif. Publi.* 1988, *89*, 372–377.

[11] Jankowiak, R., Small, G. J., *Anal. Chem.* 1989, *61*, 1023A–1032A.

[12] Devanesan, P. D., RamaKrishna, N. V. S., Todorovic, R., Rogan, E. G., Cavalieri, E. L., Jeong, H., Jankowiak, R., Small, G. J., *Chem. Res. Toxicol.* 1992, *5*, 302–309.

[13] Rogan, E. G., Devanesan, P. D., RamaKrishna, N. V. S., Higginbotham, S., Padmavathi, N. S., Chapman, K., Cavalieri, E. L., Jeong, H., Jankowiak, R., Small, G. J., *Chem. Res. Toxicol.* 1993, *6*, 356–363.

[14] Devanesan, P. D., RamaKrishna, N. V. S., Padmavathi, N. S., Higginbotham, S., Rogan, E. G., Cavalieri, E. L., Marsch, G. A., Jankowiak, R., Small, G. J., *Chem. Res. Toxicol.* 1993, *6*, 364–371.

[15] Suh, M., Ariese, F., Small, G. J., Jankowiak, R., Hewer, A., Phillips, D. H., *Carcinogenesis* 1995, *16*, 2561–2569.

[16] Jankowiak, R., Small, G. J., *Chem. Res. Toxicol.* 1991, *4*, 256–269.

[17] Todorowic, R., Ariese, F., Devanesan, P., Jankowiak, R., Small, G. J., Rogan, E. G., Cavalieri, E. L., *Chem. Res. Toxicol.* 1997, *10*, 941–947.

[18] Cavalieri, E. L., Rogan, E. G., In: Neilson, A. H. (Ed.), *The Handbook of Environmental Chemistry*, Chapter 11, Springer-Verlag, Heidelberg 1998, pp. 81–118.

[19] Chakravarti, D., Pelling, J. C., Cavalieri, E. L., Rogan, E. G., *Proc. Natl. Acad. Sci. USA* 1995, *92*, 10422–10426.

[20] Cavalieri, E. L., Rogan, E. G., *Pharm. Ther.* 1992, *55*, 183–199.

[21] Rogan, E. G., RamaKrishna, N. V. S., Higginbotham, S., Cavalieri, E. L., Jankowiak, R., Small, G. J., *Chem. Res. Toxicol.* 1990, *3*, 441–444.

[22] Jankowiak, R., Small, G. J., in: Neilson, A. H. (Ed.), *The Handbook of Environmental Chemistry*, Chapter 12, Springer-Verlag, Heidelberg 1998, pp. 119–146.

[23] Cavalieri, E. L., Rogan, E. G., *Xenobiotica* 1995, *25*, 677–688.

[24] Cheng, L., Devanesan, P. D., Higginbotham, S., Ariese, F., Jankowiak, R., Small, G. J., Rogan, E. G., Cavalieri, E. L., *Chem. Res. Toxicol.* 1996, *9*, 897–903.

[25] Devanesan, P. D., Higginbotham, S., Ariese, F., Jankowiak, R., Suh, M., Small, G. J., Cavalieri, E. L., Rogan, E. G., *Chem. Res. Toxicol.* 1996, *9*, 1113–1116.

[26] Devanesan, P. D., RamaKrishna, N. V. S., Higginbotham, S., Padmavathi, N. S., Chapman, K., Cavalieri, E. L., Jeong, H., Jankowiak, R., Small, G. J., *Chem. Res. Toxicol.* 1993, *6*, 356–363.

[27] Mumford, J. L., Li., X., Hu, F., Lu, X. B., Chuang, J. C., *Carcinogenesis* 1995, *16*, 3031–3036.

[28] Bowman, E. D., Rothman, N., Hackl, C., Santella, R. M., Weston, A., *Biomarkers* 1997, *2*, 321–327.

[29] Terabe, S., Otsuka, K., Ichikawa, K., Tsuchiya, A, Ando, T., *Anal. Chem.* 1984, *56*, 111–113.

[30] Jongeneelen, F. J., Anzion, R. B. M., Leijdekkers, C.-M., Bos, R. P., Henderson, P. T., *Int. Arch. Occupat. Environm. Health* 1985, *57*, 47–55.

[31] Geacintov, N. E., in: Harvey, E. G. (Ed.), *Polycyclic Aromatic Hydrocarbon Carcinogenesis*, American Chemical Society, Washington, DC, pp. 107–124.

[32] Schaller, K. H., Angerer, J., Hausmann, N., *Proceedings of the 13th International Symposium on Polynuclear Aromatic Hydrocarbons*, Bordeaux, France 1993, pp. 1023–1030.

[33] Lin, C.-H., Zamzow, D., Small, G. J., Jankowiak, R., *Polycyclic Aromatic Compounds* 1999, in press.